Contribution of increasing CO_2 and climate change to the carbon cycle in China's ecosystems

Qiaozhen Mu,[1] Maosheng Zhao,[1] Steven W. Running,[1] Mingliang Liu,[2] and Hanqin Tian[2]

[1]   Atmospheric CO_2 and China's climate have changed greatly during 1961–2000. The influence of increased CO_2 and changing climate on the carbon cycle of the terrestrial ecosystems in China is still unclear. In this article we used a process-based ecosystem model, Biome-BGC, to assess the effects of changing climate and elevated atmospheric CO_2 on terrestrial China's carbon cycle during two time periods: (1) the present (1961–2000) and (2) a future with projected climate change under doubled CO_2 (2071–2110). The effects of climate change alone were estimated by driving Biome-BGC with a fixed CO_2 concentration and changing climate, while the CO_2 fertilization effects were calculated as the difference between the results driven by both increasing CO_2 and changing climate and those of variable climate alone. Model simulations indicate that during 1961–2000 at the national scale, changes in climate reduced carbon storage in China's ecosystems, but increasing CO_2 compensated for these adverse effects of climate change, resulting in an overall increase in the carbon storage of China's ecosystems despite decreases in soil carbon. The interannual variability of the carbon cycle was associated with climate variations. Regional differences in climate change produced differing regional carbon uptake responses. Spatially, reductions in carbon in vegetation and soils and increases in litter carbon were primarily caused by climate change in most parts of east China, while carbon in vegetation, soils, and litter increased for much of west China. Under the future scenario (2071–2110), with a doubling CO_2, China will experience higher precipitation and temperature as predicted by the Hadley Centre HadCM3 for the Intergovernmental Panel on Climate Change Fourth Assessment. The concomitant doubling of CO_2 will continue to counteract the negative effects of climate change on carbon uptake in the future, leading to an increase in carbon storage relative to current levels. This study highlights the role of CO_2 fertilization in the carbon budget of China's ecosystems, although future studies should include other important processes such as land use change, human management (e.g., fertilization and irrigation), environmental pollution, etc.

Citation: Mu, Q., M. Zhao, S. W. Running, M. Liu, and H. Tian (2008), Contribution of increasing CO_2 and climate change to the carbon cycle in China's ecosystems, *J. Geophys. Res.*, *113*, G01018, doi:10.1029/2006JG000316.

1.   Introduction

[2]   Terrestrial ecosystems are important components of the global carbon cycle, acting as a carbon sink and slowing the increase of atmospheric CO_2 concentration resulting from human activities [*Prentice et al.*, 2001]. Although likely mechanisms for the sink are known, the relative contributions of different factors (e.g., climate variability, human activities and natural disturbances) are uncertain [*Prentice et al.*, 2001]. Studying regional variability in carbon budgets can improve our understanding of global

carbon cycle [*Sabine et al.*, 2004]. China is the third largest country in area and has the largest population (approximately 1.3 billion) in the world [*State Statistical Bureau*, 2003; *McNeill*, 2000]. Studies on changes in carbon fluxes and storages of ecosystems in China are significant both scientifically and socially.

[3]   China is a monsoon-controlled country, with climate ranging from tropical to cold temperate regions, causing China to have the most diverse climate regimes and ecosystems in the world. The Tibetan Plateau is the highest plateau in the world, further confounding climate effects in China. Since the late 19th century, the combustion of fossil fuels and deforestation have increased atmospheric CO_2 from a preindustrial level of approximately 280 ppm to 379 ppm in 2005 [*Intergovernmental Panel on Climate Change* (*IPCC*), 2007; *Keeling et al.*, 1995, also unpublished data, 2005, available at http://cdiac.esd.ornl.gov/ftp/trends/co2/maunaloa.co2]. The atmospheric CO_2 concentra-

---

[1]Numerical Terradynamic Simulation Group, College of Forestry and Conservation Sciences, University of Montana, Missoula, Montana, USA.
[2]School of Forestry and Wildlife Sciences, Auburn University, Auburn, Alabama, USA.

tion will continue to increase during the next 100 years [*IPCC*, 2007]. Meanwhile, global climate has changed greatly and will continue to change. The global average surface temperature has increased by approximately $0.74 \pm 0.18°C$ over the last 100 years (1906–2005) with 1998 ranking first of the warmest years on record in one estimate and 2006 in the other two estimates [*IPCC*, 2007]. Both global maximum and minimum temperatures are increasing, with minimum temperatures increasing at nearly twice the rate of the maximum temperature during 1950–1993 [*Karl et al.*, 1991, 1993]. On the basis of observations in China, maximum and minimum temperatures increased by $0.4°C$ and $1.4°C$, respectively, during 1951–1999 [*Zhai and Pan*, 2003]. *Zhai et al.* [1999] also found a significant increase in precipitation over the middle and lower reaches of the Yangtze River and western China during the latter part of the 20th century, while detecting a declining trend in precipitation over northern China. Increasing atmospheric CO_2 can promote ecosystem carbon sequestration [*Curtis and Wang*, 1998; *Nowak et al.*, 2004; *Ainsworth and Long*, 2005; *Graaff et al.*, 2006], while changing climate is the leading driving force responsible for the interannual atmospheric CO_2 growth rate [*Nemani et al.*, 2003]. Some modeling studies suggest that CO_2 fertilization effects be a major contributor to the "missing" carbon sink [*Gifford*, 1994; *Friedlingstein et al.*, 1995]. Other researchers have studied the separate effects of CO_2 fertilization and climate change globally or regionally [*McGuire et al.*, 2001; *Tian et al.*, 1998, 1999, 2003], but no such work has yet been done in China. Quantifying the spatial and temporal variations in terrestrial carbon balance of monsoonal China, while also separating the effects of increasing CO_2 and spatially differing changes in climate, will be of great significance for understanding mechanisms of regional and global ecosystem carbon dynamics.

[4] Recent studies suggest that China was a carbon sink with a net ecosystem production (NEP) of 70 Tg C/a during 1981–2000 [*Cao et al.*, 2003] and that terrestrial net primary production (NPP) is increasing in China at the national scale, but the magnitude differs both spatially and temporally [*Fang et al.*, 2003; *Cao et al.*, 2003]. *Fang et al.* [2001] found that China's forest biomass carbon storage increased from the mid-1970s to 1998. *Tian et al.* [2003], using the Terrestrial Ecosystem Model [*Raich et al.*, 1991; *Melillo et al.*, 1993; *Tian et al.*, 1999], found that carbon storage in terrestrial east Asia (including China, Japan, Korea, and Mongolia) has increased slowly since the 1970s and that east Asia became a carbon sink during 1980–1989 because of forest regrowth and the enhancing role of CO_2 fertilization on vegetation. For China's ecosystems, however, little is known about the long-term trend and future projected change of carbon fluxes and storages, and the individual roles of climate change and CO_2 fertilization in the carbon cycle of these ecosystems.

[5] In this study, we used a well-documented daily ecosystem process model Biome-BGC [*Running and Hunt*, 1993; *White et al.*, 2000; *Thornton et al.*, 2002] to differentiate the effects of changing climate and increasing CO_2 on the carbon cycle for terrestrial China for two time periods, 1961–2000 (present conditions), and future (2071–2110) conditions with projected climate change under doubled CO_2, while ignoring other major disturban-

ces such as (1) land use change resulting from human activities [*Tian et al.*, 2008], (2) disturbances such as fires [*Lü et al.*, 2006; *Running*, 2006], and (3) environmental pollution as aerosols [*Bergin et al.*, 2001], nitrogen deposition [*Sala et al.*, 2000] and O_3 [*Karnosky et al.*, 1999, 2002]. The objectives of this paper are to (1) study the long-term changes of terrestrial carbon cycle components in China since 1961; (2) determine the effects of both CO_2 fertilization and the changing climate on the terrestrial carbon cycle of China; and (3) predict the potential change in future carbon storage with both projected climate change and doubled CO_2.

2. Data and Methods

2.1. Biome-BGC Model

[6] Biome-BGC (version 4.1.2) is a process-based ecosystem model, requiring prescribed vegetation and site conditions, meteorology, and vegetation-specific parameter values to simulate daily fluxes and states of energy, carbon, water, and nitrogen for the vegetative and soil components of terrestrial ecosystems [*Running and Hunt*, 1993; *White et al.*, 2000; *Thornton et al.*, 2002]. Processes in Biome-BGC depend strongly on the history of weather conditions, or climate. Biome-BGC uses a daily time step to take advantage of widely available daily temperature and precipitation data, from which daylight average shortwave radiation, vapor pressure deficit, and temperature are estimated using the MT-CLIM model [*Running and Hunt*, 1993; *White et al.*, 2000; *Thornton et al.*, 2002].

[7] The plant canopy leaf area is divided into sunlit and shaded fractions, and solar energy is distributed between these fractions using a radiation extinction coefficient that varies with leaf geometry. For C3 plants, carbon assimilation on a unit projected leaf area basis is estimated independently for the sunlit and shaded canopy fractions, using a biochemical model [*Farquhar et al.*, 1980, 2001] modified by (1) kinetic parameters from *Woodrow and Berry* [1988] and *De Pury and Farquhar* [1997] and (2) biochemical parameters from *Wullschleger* [1993]. The rate of photosynthesis is determined by the intercellular CO_2 concentration, the rate of carboxylase activity, and the rate of electron transport. Intercellular CO_2 concentration depends on both atmospheric CO_2 concentration and leaf-level conductance as CO_2 is transferred from the atmosphere into the leaf via diffusion through the stomata. As atmospheric CO_2 increases, intercellular CO_2 levels also increase [*Thornton*, 1998], thus potentially increasing assimilation. Assimilation is then limited by either the rate of carboxylase activity or the rate of electron transport, whichever is smaller. In the absence of recent disturbance events, an increasing sink strength due to CO_2 fertilization depends mostly on an increasing concentration of atmospheric CO_2 [*Thornton et al.*, 2002; *Nowak et al.*, 2004].

[8] NPP is the residual of gross primary production (GPP) minus maintenance and growth respiration. Gross primary production is the sum of assimilation from the sunlit and shaded portions of the canopy. Maintenance respiration is calculated as a function of tissue mass, tissue nitrogen concentration and tissue temperature [*Ryan*, 1991], and occurs regardless of current assimilation rate. Growth respiration is calculated separately for woody and non-
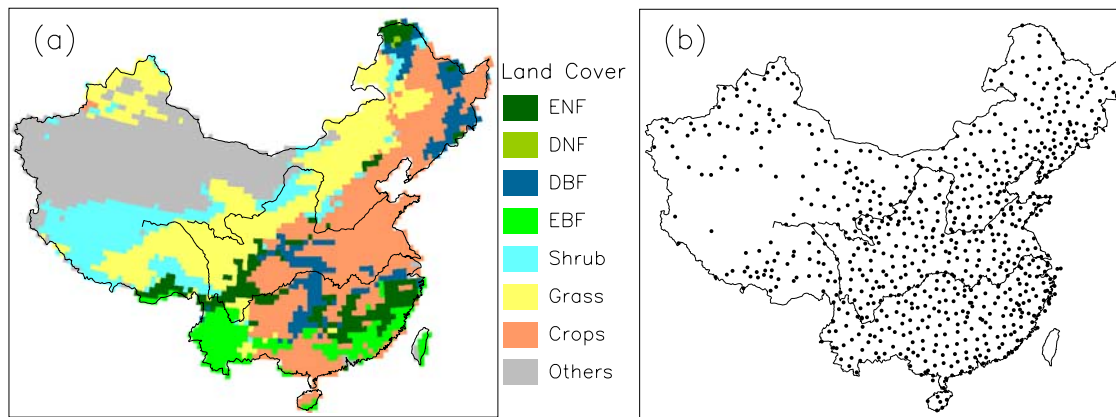
Figure 1. (a) Land cover types in China (latitude 17.5°, 52.5°; longitude 80.5°, 128°) from MODIS 12Q1, land cover type 5: DBF, deciduous broadleaf forest; DNF, deciduous needleleaf forest; EBF, evergreen broadleaf forest; ENF, evergreen needleleaf forest. Other cover types are barren or sparsely vegetated, urban and built up, snow and ice, and unclassified. Crops are treated as grass in Biome-BGC. (b) Distribution of weather stations in China used in the study.

woody tissues, and is assumed to be constant for each of them. Total growth respiration is calculated by multiplying the appropriate constant by the new growth, which is based on the current assimilation rate. NPP consists of both the aboveground (leaves, stems) and belowground (roots) production.

[9] New carbon is allocated to new leaf and other plant tissues as fine roots, live and dead stem wood, live and dead coarse root wood. Before entering the active litter pools, woody litter passes through a coarse wood debris pool that is subject only to physical degradation [*Thornton et al.*, 2002]. Litter and soil organic carbon (SOM) decomposition produces a heterotrophic respiration flux, which depends on the size of the litter and SOM pools and their decomposition rate constants. These rate constants depend on soil temperature and soil moisture [*Lloyd and Taylor*, 1994].

2.2. Input Data Sets
2.2.1. Land Cover
[10] Biome-BGC uses a suite of parameters to differentiate biomes on the basis of their ecophysiological characteristics. The vegetation data (Figure 1a) is based on land cover Type 5 from the 1-km resolution Moderate Resolution Imaging Spectroradiometer (MODIS) land cover data set (Collection 4) [*Friedl et al.*, 2002] (see also A. Strahler et al., MODIS land cover product algorithm theoretical basis document (ATBD) version 5.0. MODIS land cover and land-cover change, 1999, 72 pp., available at http://modis.gsfc.nasa.gov/data/atbd/atbd_mod12.pdf), which we condensed into six land cover types used in Biome-BGC (deciduous broadleaf forest (DBF), deciduous needleleaf forest (DNF), evergreen broadleaf forest (EBF), evergreen needleleaf forest (ENF), C3 grasses, C4 grasses, and evergreen shrubs). Crops, urban and built-up areas, snow and ice, barren, sparsely vegetated, or unclassified pixels in MODIS land cover type 5 were treated as grass in Biome-BGC. Discrimination between C3 and C4 grasses is based on the mean annual daytime average temperature; if the average temperature is less than or equal to 10°C, grass is treated as C3 grass, otherwise, it is modeled as C4 grass [*Sims and Risser*, 1999]. We then aggregated 1-km data into 0.5° on the basis of the

dominant land cover types to be consistent with spatial resolution of the meteorological data set described below.

[11] Since Biome-BGC cannot simulate changes in biome geographic distribution, the same vegetation map is used for both the current and future scenarios. Thus we ignore potential shifts in biome distribution under projected climate change as predicted by biogeography models [e.g., *Zhao et al.*, 2002].

2.2.2. Meteorology Data
[12] The primary driving variables for estimating ecosystem processes with Biome-BGC are the daily meteorological data, including precipitation (PREC), solar radiation (SRAD), daytime average vapor pressure deficit (VPD), maximum temperature (Tmax), minimum temperature (Tmin), daytime average temperature (Tday) and day length (DAYL). The daily gridded meteorology data for 1961–2000 at 0.5° latitude/longitude resolution over China were generated using the DAYMET algorithm [*Thornton and Running*, 1999; *Kimball et al.*, 1997; *Thornton et al.*, 1997] with observed daily PREC, Tmax and Tmin from 740 weather stations (Figure 1b). Downward solar radiation is semiempirically retrieved with physical laws and the empirical relationship between clear sky radiation and cloudy sky radiation on the basis of latitude, Julian day, diurnal temperature range, precipitation and air humidity [*Thornton and Running*, 1999]. There are no available weather data from Taiwan and only a few stations in western China, especially on the Tibetan Plateau, Xinjiang and Qinghai. The paucity of distributed weather stations in these remote areas likely introduces errors to gridded daily meteorology data, possibly creating some bias in the simulated results in these corresponding areas by Biome-BGC.

[13] Future projected climate data under doubled CO₂ were obtained by combining the monthly climate change simulated by Hadley Centre HadCM3 for the IPCC Fourth Assessment with the observed daily climate during 1961–2000. The future monthly climate change is from the last 40-year (2071–2110) results of a scenario, i.e., 1%/a CO₂ increase to doubling. The projected monthly climate change under this scenario was the relative difference or ratio to the

modeled present climate, the last 40 years of 20th Century experiment (20C3M). Details of these HadCM3 experiments are at (http://www-pcmdi.llnl.gov/ipcc/standard_output.html). We used the climate simulation results from HadCM3 because predecessor HadCM2 performed best among all GCMs in simulating climate in China during 1961–1990 for the IPCC's Third Assessment Report [IPCC, 2001; Zhao et al., 2002]. To obtain projected VPD, saturated vapor pressure (SVP) was calculated for the two periods using the corresponding temperature. Because a wide variety of GCMs suggest that it is realistic to assume relative humidity (RH) will not change as climate changes [Allan et al., 2003; Ingram, 2002; Seneviratne et al., 2002; Ye et al., 1998], we assume that RH will not change in the future. The VPD was calculated using SVP*(1.0-RH). Then, the differences combined with the present observed climate (1961–2000) were used to represent for future climate. In this case, future VPD will increase with increasing temperature, and the VPD constraints on NPP will be higher in the future. Though Roderick and Farquhar [2002] found that VPD has remained nearly constant during the past 50 years in spite of increases in average temperature, we found VPD over most parts of China has been increasing during 1961–2000. For future daily precipitation, we first calculated the ratio of future monthly precipitation under doubled CO$_2$ to the monthly precipitation of the last 40 years of 20C3M as simulated by HadCM3. Then this monthly ratio was multiplied with the observed daily precipitation during 1961–2000 to get the future daily precipitation.

2.2.3. Atmospheric CO$_2$ and Other Ancillary Data

[14] For the period 1961–2000, atmospheric CO$_2$ concentrations were obtained from observations taken at Mauna Loa [Keeling et al., 1995, also unpublished data, 2005, available at http://cdiac.esd.ornl.gov/ftp/trends/co2/maunaloa.co2]. Future CO$_2$ (740 ppm) is doubling the CO$_2$ concentration of 2000. Since we calculated future climate using projected future climate change together with observed climate during 1961–2000, the average CO$_2$ concentration during 1961–2000 was used as the baseline CO$_2$ level for the future to detect the effects of doubled CO$_2$ on China's terrestrial ecosystems (see §2.3).

[15] Site conditions include soil texture, elevation, and latitude. Soil texture data, including sand/silt/clay percentages and effective soil depth, were developed using data from the 1:1,000,000 soil type data set and the second national soil inventory of China [Zhang et al., 2005; Wang et al., 2003]. Elevation data was integrated from China's national 1:250,000 digital elevation model (DEM) data. All these spatial data were then smoothed to 0.5° spatial resolution.

2.3. Methodology

[16] To test the performance of Biome-BGC in simulating the CO$_2$ fertilization effects, we ran Biome-BGC under elevated CO$_2$ and compared the results with those from field experiments (e.g., recent free air CO$_2$ enrichment (FACE) experiments by Norby et al. [2005]). First, a spin-up run was used to bring the model state variables into steady state with meteorology for 1961–2000 and a CO$_2$ concentration of 376 ppm for each pixel. At this steady state, there is still variation resulting from interannual

variability in the weather record, but the long-term mean fluxes are stationary, and the long-term mean net ecosystem carbon exchange (NEE) is zero. The main purpose of the spin-up run is to bring SOM into dynamic equilibrium for the specified climate and vegetation type. Since SOM accumulates as a result of litter decomposition and the mineralization of SOM provides most of the nitrogen required for new plant growth, there are strong feedbacks between the development of plant and soil pools of carbon and nitrogen. The average typical spin-up time is about 2000 simulation years [White et al., 2000; Thornton et al., 2002]. Using the spin-up endpoint as an initial condition, the 1961–1995 period was simulated with the changing 1961–1995 meteorology and fixed CO$_2$ at 376 ppm for each pixel. We then constructed two sets of simulation sequences from 1996 to 2000 with (1) CO$_2$ at 376 ppm and (2) CO$_2$ at 550 ppm, respectively, to be consistent with the ambient and elevated CO$_2$ concentrations in the FACE experiments reported by Norby et al. [2005]. The two sets of 5-year (1996–2000) average NPP were then analyzed (section 3).

[17] To ascertain the separate effects of CO$_2$ fertilization and climate change on China's terrestrial carbon cycle, two sets of simulations were designed for both the present and future. For the present, there are two experiments: (1) CO2Var (i.e., the control run), driven by the present meteorology and variable CO$_2$ concentration and (2) CO2Fix, which was simulated using a fixed CO$_2$ concentration of 317.63 ppm (the value in 1961) and changing climate. CO2Var estimates the carbon cycle of terrestrial China during 1961–2000. The effects of climate change alone on the carbon cycle were obtained from the results simulated from CO2Fix, and CO$_2$ fertilization effects were estimated as the difference between the two simulations (CO2Var – CO2Fix). Similarly, for the future scenario, two corresponding experiments were conducted driven by the future climate (2071–2110): (1) CO22X (the control run), which was simulated with a CO$_2$ concentration (740 ppm) double of that in 2000 and (2) CO21X, which was driven by the average CO$_2$ concentration for 1961–2000. The difference between CO22X and CO2Var reveals how the carbon cycle will change under the projected climate and doubled CO$_2$ in the future relative to the present, and the CO$_2$ effects in the future were estimated from these two simulations (CO22X – CO21X). Comparisons of present and future carbon cycles were used to predict the future carbon storage change in terrestrial China.

[18] In our study, croplands and barren areas were simulated as grass, and we admit such treatment will introduce biases in the results. While Wang et al. [2005] have developed a cropland Biome-BGC for a specific site with availability of detailed management information such as irrigation, it is challenging to obtain the necessary irrigation and fertilizer data for all of the agricultural lands of China. Moreover, we ignored the effects from the management practices such as nitrogen fertilization, pesticide applications, and irrigation because (1) the current Biome-BGC has no module to simulate these effects regionally; (2) the spatial data for these managements are inadequate or unavailable; and (3) the objective of our study is to identify
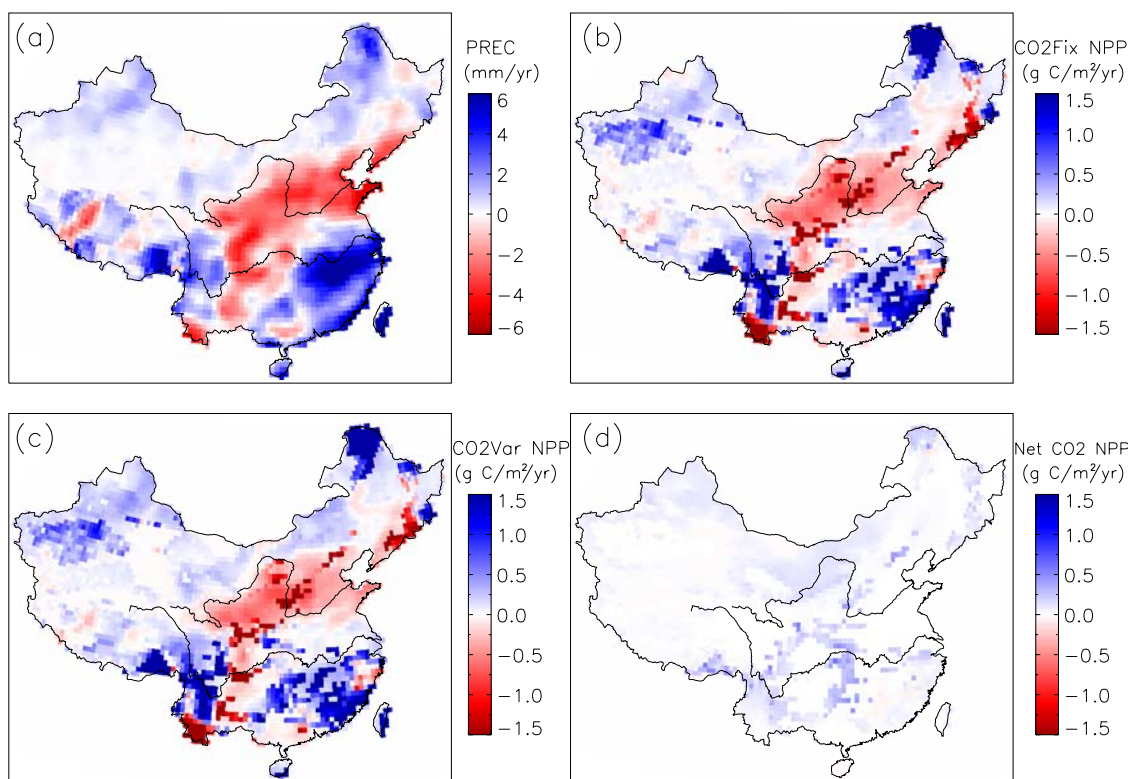
Figure 2. The 0.5° spatial trends of (a) observed precipitation (PREC) and NPP estimated by Biome-BGC during 1961–2000 driven by (b) fixed CO_2 (at 1961 level) and variable meteorology data (CO2Fix NPP) and (c) variable CO_2 concentration and meteorology (CO2Var NPP). (d) Net CO_2 fertilization effects (Net CO2 NPP); net CO_2 effects are calculated as the difference between CO2Var and CO2Fix.

the different effects of changing climate and atmospheric CO_2 on ecosystem carbon storages.

3. Results

[19] For the 696 forest pixels in China (Figure 1a), the stimulated NPP under the elevated CO_2 of 550 ppm is 7.87 ± 3.45% higher than that under ambient CO_2 (376 ppm), which is smaller than the recent reported 23 ± 2% from four FACE experiments [*Norby et al.*, 2005]. There are several reasons that the CO_2 fertilization effects estimated by Biome-BGC may be lower. First, though *Norby et al.* [2005] concluded that the CO_2 fertilization effects were conserved for these young trees, *DeLucia et al.* [2005] reported that there was discrepancy in the NPP response to CO_2 enrichment between two young forest sites, with a 24% increase for Duke site and 18% for ORNL site. In their review, *Nowak et al.* [2004] found the NPP at different FACE sites varied, with a mean increase of 20% at 550 ppm. At two large-scale replicated FACE facilities, the effects of elevated CO_2 on yields of C3 crops showed overall smaller increases than were expected on the basis of earlier enclosure studies [*Ainsworth and Long*, 2005]. Secondly, the data for Norby et al.'s and DeLucia et al.'s analyses come from four planted, fast-growing young (<30-year) temperate forests. *Wittig et al.* [2005] report a tremendous decline in GPP stimulation from planting to canopy closure in a FACE experiment for young trees. Most recently, a FACE exper-

iment for ca. 100-year-old mature temperate forest trees showed that most of species had no growth response to elevated CO_2 for the initial 4-year experiment [*Asshoff et al.*, 2006]. There are a number of uncertainties in the FACE experiments resulting from tie sites and the FACE technology itself [*Ainsworth and Long*, 2005], which may lead to differences in FACE results. Finally, Biome-BGC is an ecosystem equilibrium model, which does not include the age-dependent photosynthesis rates [*Thornton et al.*, 2002; *Lewis et al.*, 2002], and NPP is the balance between GPP and plant respiration. Uncertainties in plant respiration may introduce biases in NPP estimates since we do not yet fully understand plant respiration [*Amthor*, 2000]. In addition, China's ecosystems and climate are different from those in the USA. Therefore it would be inappropriate to conclude that Biome-BGC underestimates the CO_2 fertilization effects on China's ecosystems.

3.1. Carbon Budget and Climate During 1961–2000

[20] We analyzed different carbon flux variables including NPP, soil heterotrophic respiration (Rh), NEP, and NEE from Biome-BGC to explore impacts of changes in the atmosphere and climate on the China's ecosystem primary production and carbon fluxes. We also analyzed different carbon state variables (i.e., carbon storage) for different components, including vegetation (Cveg), litter (Clitr), soil (Csoil), and total (Ctot) carbon storage. The changes in the carbon storage can reveal the capacities of carbon storage by China's ecosystems and the role (sink or source of
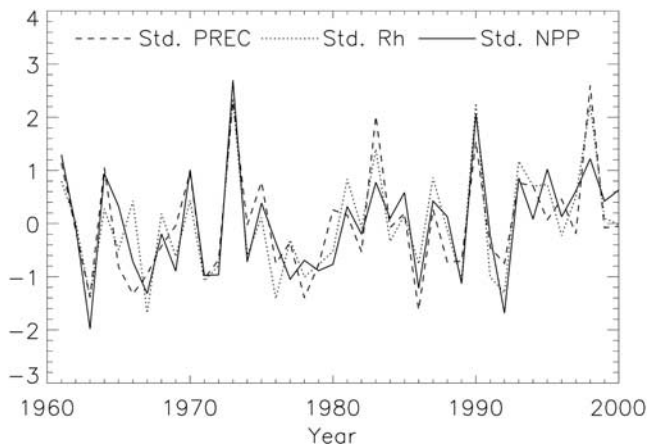
Figure 3. Variations in standardized annual observed precipitation (Std. PREC, dashed line), standardized Biome-BGC estimated annual soil heterotrophic respiration (Std. Rh, dotted line), and annual net primary production (Std. NPP, solid line) across China during 1961–2000 from CO2Var.

carbon) which they could be playing in the global carbon cycle. Without specific notification, the results and discussion in the following sections are from the simulation driven by both the variable CO_2 and climate (i.e., CO2Var).

3.1.1. Long-Term Change in Climate and Carbon Fluxes at the National Scale

[21] During 1961–2000, China's climate showed considerable variability with modest positive trends in maximum temperature (0.018°C/a, $p = 0.0002$), daytime average temperature (0.023°C/a, $p < 0.0001$), minimum temperature (0.036°C/a, $p < 0.0001$), and VPD (0.646 Pa/a, $p = 0.01$), along with a negative trend in solar radiation (−1.5493 MJ/m²/a, $p = 0.001$). The trends of increasing temperatures are consistent with those of *Zhai and Pan* [2003], and the decreasing solar radiation agrees with the observed trends from weather stations [*Kaiser and Qian*, 2002]. There was also a positive, but insignificant, trend in annual precipitation (0.43 mm/a, $p > 0.12$). The spatial pattern of the precipitation trend is similar to that of *Zhai et al.* [1999] although our study occurs during a slightly different time period (Figure 2a).

[22] Figure 3 shows the interannual variability (shown in standardized values) of mean annual precipitation and estimated total annual carbon cycle components (NPP and Rh) at the national scale. Interannual variations in the modeled total NPP and Rh were tightly coupled to variations in precipitation. For the 40-year period, there was a strong positive correlation between interannual precipitation and NPP ($R^2 = 0.6545$, $p < 0.0001$), Rh ($R^2 = 0.6953$, $p < 0.0001$) (Figure 3). The correlations of NPP and Rh with temperature are much lower than with precipitation. Thus precipitation is the dominant climate factor for vegetation primary production in China, agreeing with published reports [*Cao et al.*, 2003], and increasing precipitation is partly responsible for the increasing NPP and Rh at the national scale.

[23] At the national scale, our results of NEP agree with *Cao et al.*'s [2003] findings that NEP is positive with an average of 160 Tg C/a ranging from 70 Tg C/a to 230 Tg C/a. However, the trend of NEP is negative because Rh is increasing more rapidly than NPP. Table 1 indicates that both Rh and NPP had a similar increasing trend of approximately +1.5 Tg C/a, with a slightly higher rate of Rh than NPP, resulting in a small decreasing trend of NEP at −0.02 Tg C/a. Although the magnitudes in the NEP average and trend are different from *Cao et al.*'s [2003] (1981–2000 NEP average of 70 Tg C/a, with a decreasing rate of −1.0 Tg C/a), the direction of change is the same, which indicates that the capacity of carbon uptake of China's ecosystems was decreasing during 1961–2000.

[24] There is a simple fire disturbance module in Biome-BGC. Each year, the vegetation mortality fraction through fire is a constant for each biome type [*Thornton et al.*, 2002], and the NEE is the difference between NEP and the carbon loss through fire (positive NEE means net carbon sink, negative means carbon source). The sum of NEE (373.5 Tg C) during 1961–2000 is the total net carbon fixed by China's ecosystems, i.e., to the total carbon pool, with an average of 9.3 Tg C/a. During 1961–2000, China's ecosystems were a carbon sink with changing climate and CO_2, but without considering the land use change, real fire disturbance, aerosol, nitrogen deposition or human management.

3.1.2. CO₂ Fertilization Effects and Interannual Variation in the Carbon Storage

[25] For each year of the two experiments (CO2Fix and CO2Var), we calculated the carbon storage of several different carbon pools, including Cveg, Clitr, Csoil and Ctot. The Ctot of terrestrial China was 158.9 Pg C averaged over 1961–2000, with 70.8 Pg C of Cveg, 14.3 Pg C of Clitr, and 73.8 Pg C of Csoil (Figure 4).

[26] Figure 5 shows the time series of carbon storage anomalies from the two simulations relative to their corresponding averages during 1961–2000. CO2Fix shows that, from 1961 to 2000, climate change alone reduced Cveg by −114.8 Tg C, Csoil by −20.3 Tg C, and increased Clitr by 1.5 Tg C, and the Ctot was reduced by −133.6 Tg C at a rate of −5.3 Tg C/a (Table 1 and Figure 6), indicating that climate change decreased the capacity of carbon storage in China. The reason for the reduction in carbon storage induced by climate change alone is that, although the increasing precip-

Table 1. Annual Trends of Carbon Storages and Fluxes During 1961–2000 at the National Scale in China From Two Different Biome-BGC Experiments[a]

Variables	Experiments		Net CO₂ Effects
	CO2Fix	CO2Var	
Cveg trend, Tg C/a	−3.7	1.1	4.8
Clitr trend, Tg C/a	−1.0	6.5	7.5
Csoil trend, Tg C/a	−0.6	−0.4	0.2
Ctot trend, Tg C/a	−5.3	7.2	12.5
NPP trend, Tg C/a	1.1	1.5	0.4
Rh trend, Tg C/a	1.5	1.5	0.0
NEP trend, Tg C/a	−0.5	−0.02	0.48

[a]The carbon storage components include vegetation carbon (Cveg), litter carbon (Clitr), soil carbon (Csoil), and total carbon (Ctot), while carbon fluxes include NPP, Rh, and NEP. Biome-BGC simulations consist of CO2Fix (fixed CO_2 concentration at 1961 level and variable meteorology data) and CO2Var (variable CO_2 concentrations and meteorology data). See Figures 5 and 6.
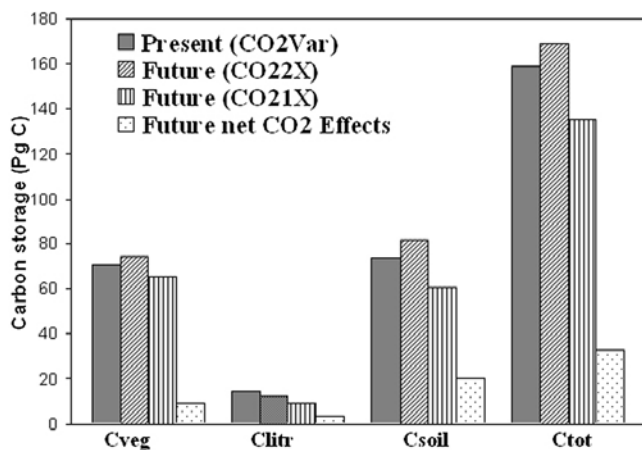
Figure 4. Vegetation (Cveg), litter (Clitr), soil (Csoil), and total carbon (Ctot) storage (Pg C) at present (1961–2000) from CO2Var and in the future from two Biome-BGC simulations: CO21X (fixed CO_2 as the average during 1961–2000) and CO22X (doubled CO_2) together with projected future climate under doubled CO_2. Future net CO2 effects are calculated as the difference between CO22X and CO21X.

itation benefited photosynthesis (i.e., increased GPP and increased NPP at a rate of 1.1 Tg C/a, Table 1), increasing temperature increased the rate of Rh (1.5 Tg C/a, Table 1) (similar to results from *Lloyd and Taylor* [1994] and *Cao et al.* [2003]), counteracting the favorable effects of increasing precipitation and hence leading to a decreasing NEP rate of −0.5 Tg C/a (Table 1), a negative sum of NEE (−58.8 Tg C), and decreasing Ctot of −133.6 Tg C from 158.77 Pg C in 1961 to 158.63 Pg C in 2000 at a rate of −5.3 Tg C/a (Table 1 and Figures 5d and 6).

[27] When stomata are open and atmospheric CO_2 is higher than normal, more CO_2 will be absorbed and fixed by vegetation because of enhanced photosynthesis. During 1961–2000, on average, CO2Var leads to a Ctot that is 188.7 Tg C higher than that from climate change alone (CO2Fix) (Figure 5d). The CO_2 fertilization effects, esti-mated as the difference between CO2Var and CO2Fix, canceled the adverse effects of climate change, enhancing terrestrial China Ctot by 459.7 Tg C at a rate of 12.5 Tg C/a during 1961–2000 (Table 1 and Figure 6). Both CO2Fix and CO2Var used the same initial condition, and hence the carbon storage in the first year (1961) was the same, while different for other years. As a result, in 1961, the value of the Net CO_2 Effects (CO2Fix − CO2Var) was 0.0 Tg C (Figure 5), while the two simulations had different anoma-lies because of different average values.

[28] Figure 5 also shows that the two experiments had strong interannual variability in carbon storage, which was
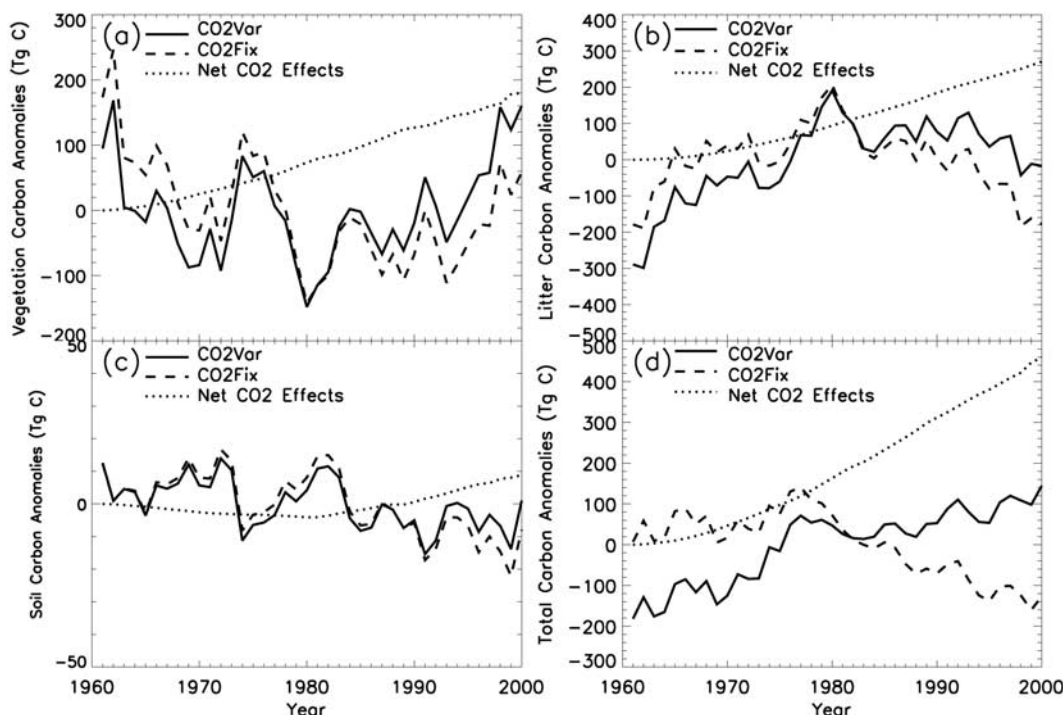
Figure 5. Anomalies of terrestrial carbon storage in (a) vegetation, (b) litter, (c) soil, and (d) total carbon during 1961–2000 in China as estimated by Biome-BGC from two different simulations: CO2Fix (fixed CO_2 concentration at 1961 level and variable meteorology data, dashed lines) and CO2Var (variable CO_2 concentration and meteorology, solid lines) relative to their corresponding averages over 1961–2000. The averages differ for each simulation, resulting in different anomaly values in 1961. Net CO_2 effects (dotted lines) are calculated as the difference between CO2Var and CO2Fix, and the curve always starts at 0 in 1961 because CO2Fix and CO2Var use the same initial soil carbon conditions and have the same values in 1961.
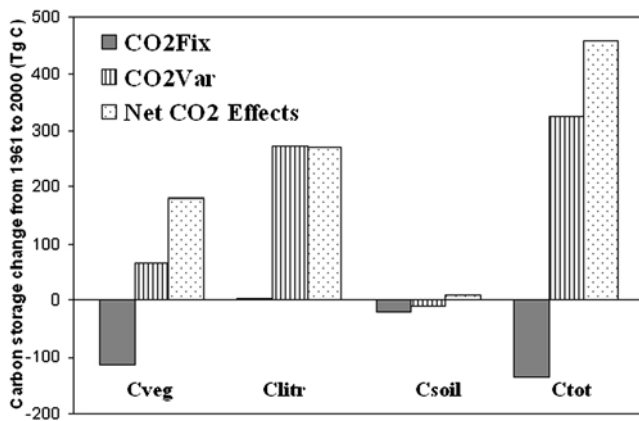
Figure 6. Carbon storage change in vegetation (Cveg), litter (Clitr), soil (Csoil), and total carbon (Ctot) (Tg C) from 1961 to 2000 simulated by Biome-BGC from CO2Fix and CO2Var. Net CO_2 effects are calculated as the difference between CO2Var and CO2Fix.

induced by interannual variations in the observed climate. The CO_2 fertilization effects contributed almost no interannual variability in the carbon storage, but did affect trends in carbon storage (Net CO_2 Effects, Figures 5 and 6). When climate change and increased CO_2 were combined (CO2Var), the interannual variability of total carbon was caused primarily by variations in observed climate, and the CO_2 fertilization alleviated or reversed the reduced trends in carbon storage caused by climate change alone. *Fang et al.* [2001] attributed the forest carbon storage increase from mid-1970s to 1998 to forest expansion, regrowth and management (afforestation and reforestation), while our results reveal CO_2 fertilization may also be an important contributor.

[29] In contrast to increases in Cveg, Clitr and Ctot, the Csoil storage (Figures 5 and 6 and Table 1) decreased by −11.5 Tg C from 1961 to 2000. This decreasing Csoil trend (Figures 5c and 6) agrees with the study of *Wang et al.* [2003] that China's soil carbon decreased from 93 Pg C in the 1960s to 92 Pg C in the 1980s, as determined by the first and second national soil surveys of China. The difference in magnitude between modeled and observed Csoil may lie in (1) uncertainties in Biome-BGC; (2) treatment of crops as grasses in our simulations; and (3) existing uncertainties in the observed soil data as discussed elsewhere [*Wang et al.*, 2003]. The modeled decline in Csoil is caused by the simulated increase in Cveg and leaf area index (LAI, $p <$ 0.0001), leading to a significant increase in evapotranspiration ($p < 0.0001$), and resulting in a significant reduction in estimated soil water ($p < 0.0001$). Consequently, this led to a significant decrease in the modeled transfer rate ($p <$ 0.0001) from litter carbon to soil carbon. During 1981– 1991, modeled soil water decreased in eastern China, which agrees with observed decreases in soil moisture found by *Ma* [1999] for the same period.

3.1.3. Dynamic Spatial Changes in the Carbon Cycle

[30] Water, solar radiation, and temperature interact to impose complex and varying limitations on vegetation activity in different parts of the world [*Churkina and Running*, 1998]. China is a monsoon country with diverse

climate regimes, biome types and complicated topography. Large differences exist in regional changes in climate and carbon cycle components. The responses of ecosystems to changes in climate and atmosphere differ by region, and therefore spatial analyses are crucial to understanding the mechanisms of regional terrestrial carbon cycle.

[31] From 1961 to 2000, over most areas of China, precipitation increased (Figure 2a). The areas with decreased precipitation were located around Shandong Peninsula, including parts of the northeastern China plain and of the southwestern China (Figure 2a). Regardless of the CO_2 effects (Figure 2d), the spatial patterns of NPP trends with fixed and variable CO_2 are nearly the same (Figures 2b and 2c), with areas of increasing NPP coinciding almost exactly with those areas of increasing precipitation (Figure 2a), further confirming that precipitation is the dominant climate factor for the vegetation primary production in China (section 3.1.1) [*Cao et al.*, 2003]. The CO_2 fertilization effects enhanced NPP almost for all regions (Figure 2d). Increasing CO_2 stimulated GPP (positive CO_2 effects on GPP all over China), but might drive higher increases in the maintenance respiration than in GPP for a few pixels, resulting in negative CO_2 effects on NPP (Figure 2d).

[32] The only area with significant and positive correlation between temperatures and NPP was in the cold Xing-An-Ling area in northeast China. For this area, during 1961–2000, temperatures had a significant increasing trend (ca. 2°C/40 a). The increasing temperatures reduced the number of days with frozen soil water, increased the days of thaw, and lengthened the growing season [*White et al.*, 1997; *Running and Kimball*, 2005], thereby enhancing photosynthesis [*De Pury and Farquhar*, 1997] and carbon uptake. In this area, the main vegetation type is DNF, specifically, boreal larch (Figure 1a). Our results are consistent with the findings of *Black et al.* [2000] and *Chen et al.* [2006] that, for boreal deciduous or evergreen needle forests, warmer years have higher carbon uptake than normal years on the basis of flux tower measurements.

[33] For some areas, driven by the fixed CO_2, the spatial pattern of Ctot change from 1961 to 2000 (Figure 7j) is opposite to that of NPP trend, especially in parts of south China and the Xing-An-Ling area (Figure 2b). The main reasons for the increasing NPP in these regions were increased precipitation (Figure 2a) and also the increased temperatures in the cold Xing-An-Ling area. At the same time, increasing precipitation and temperature (1) caused more sequestered carbon to be allocated to dead stems and dead coarse roots than to live vegetation carbon, creating more coarse wood debris as litter carbon and less vegetation carbon storage (Figure 7a); (2) enhanced the decomposition rate of litter to soils for some areas such as Xing-An-Ling area, resulting in the decreased Clitr (Figure 7d) despite more carbon converted to litter; and (3) increased Rh with a much higher rate than that of decomposition from litter carbon to soil carbon, generating decreased Csoil (Figure 7g). Consequently, Ctot was decreased in these regions (Figure 7j) driven by the variable climate alone.

[34] In general, the CO_2 effects on NPP (Figure 2d) cause more carbon be stored in vegetation (Figure 7c) and litter (Figure 7f). On the other hand, compared to the fixed CO_2, the enhanced NPP and LAI by the CO_2 fertilization effects increased evapotranspiration, led to relatively lower soil
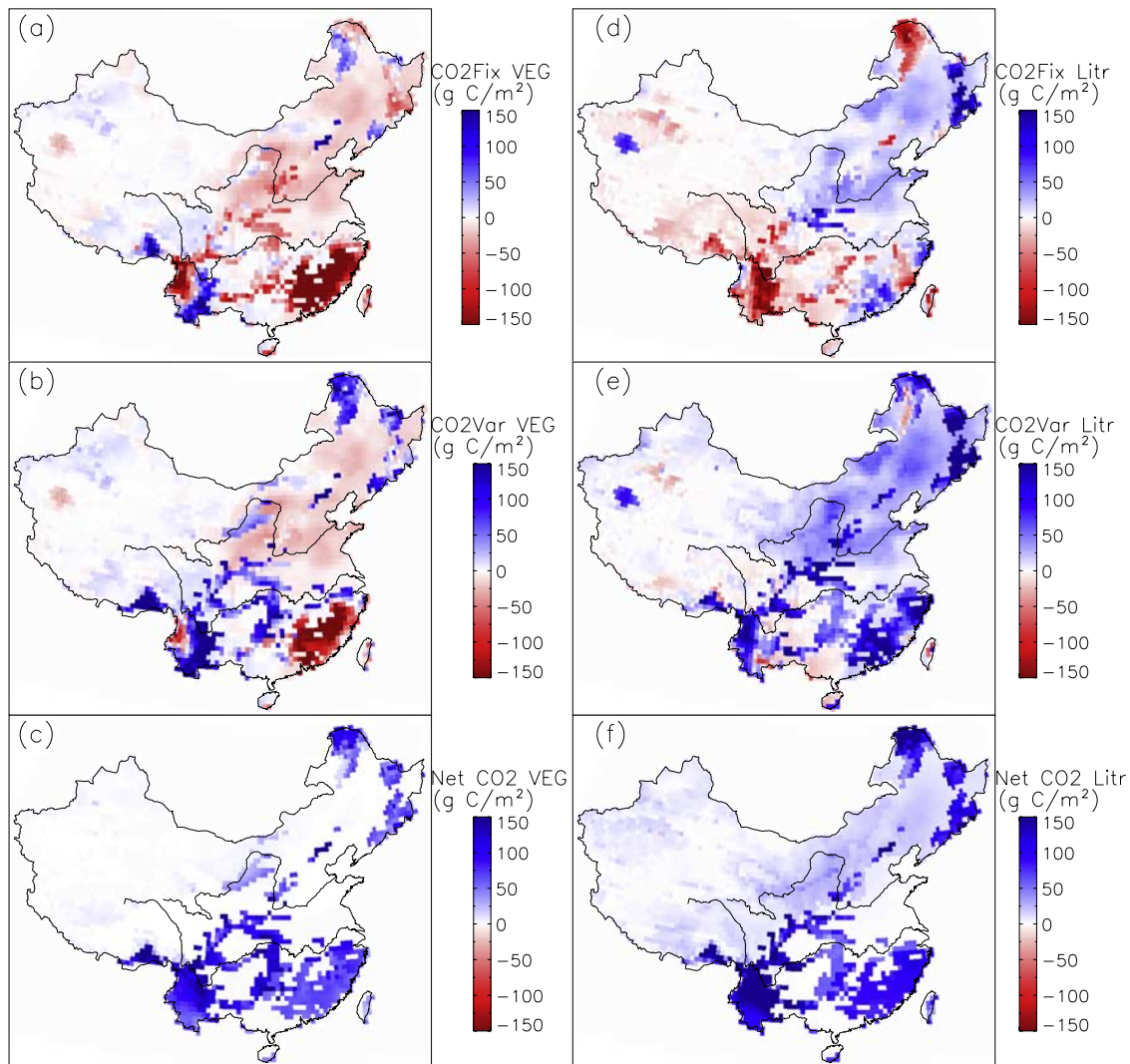
Figure 7. Spatial terrestrial vegetation carbon storage (VEG), litter carbon storage (Litr), soil carbon storage (Soil), and total carbon storage (Ctot) change in China from 1961 to 2000 as estimated by Biome-BGC: (a, d, g, and j) change from CO2Fix, (b, e, h, and k) change from CO2Var, and (c, f, i, and l) change induced by net CO$_2$ fertilization effects (Net CO2). Net CO$_2$ effects are calculated as the difference between CO2Var and CO2Fix.

moisture, and hence reduced the decomposition rate of litter to soil carbon, resulting in negative CO$_2$ effects on Csoil for most parts of China (Figure 7i). Generally, the CO$_2$ effects on Ctot are positive (Figure 7l) in most parts of China.

[35] To examine the differences in the responses of different vegetation types to the CO$_2$ fertilization, we calculated the average NPP of the two experiments (CO2Var and CO2Fix) and the net CO$_2$ effects on NPP as the difference between the NPP averages over all the pixels for forest, shrub, grass, and desert from the two experiences. Figure 8 shows the percentage of the NPP difference to the NPP average from CO2Var. On average, the NPP enhancement by the CO$_2$ fertilization effects was greatest in deserts, lowest in grasslands with shrub and forest intermediate, which generally agrees with the FACE results [*Nowak et al.*, 2004].

3.2. Carbon Cycle With Future Projected Climate Under Double CO$_2$

[36] In the future, under a doubled CO$_2$ scenario, both precipitation and temperature will increase over entire China as predicted by Hadley Centre HadCM3 (Figure 9).

3.2.1. Effects of CO$_2$ Fertilization on the Carbon Cycle at the National Scale

[37] The effects of climate change and CO$_2$ fertilization on the carbon cycle in the future (2071–2110) are similar to those in the present (1961–2000). For CO21X, NPP and Rh will be higher (54.88 Tg C/a, 67.54 Tg C/a, respectively) and NEP will be smaller (−11.66 Tg C/a) than at present (Table 2). Future climate change will deteriorate China's ecosystems, resulting in reduced Cveg, Clitr, Csoil, and Ctot when compared to values of 1961–2000 (Figure 4 and Table 2). However, for CO22X, the effects of CO$_2$ fertilization will compensate for the adverse effects of projected climate, enhancing photosynthesis, leading to an increase in
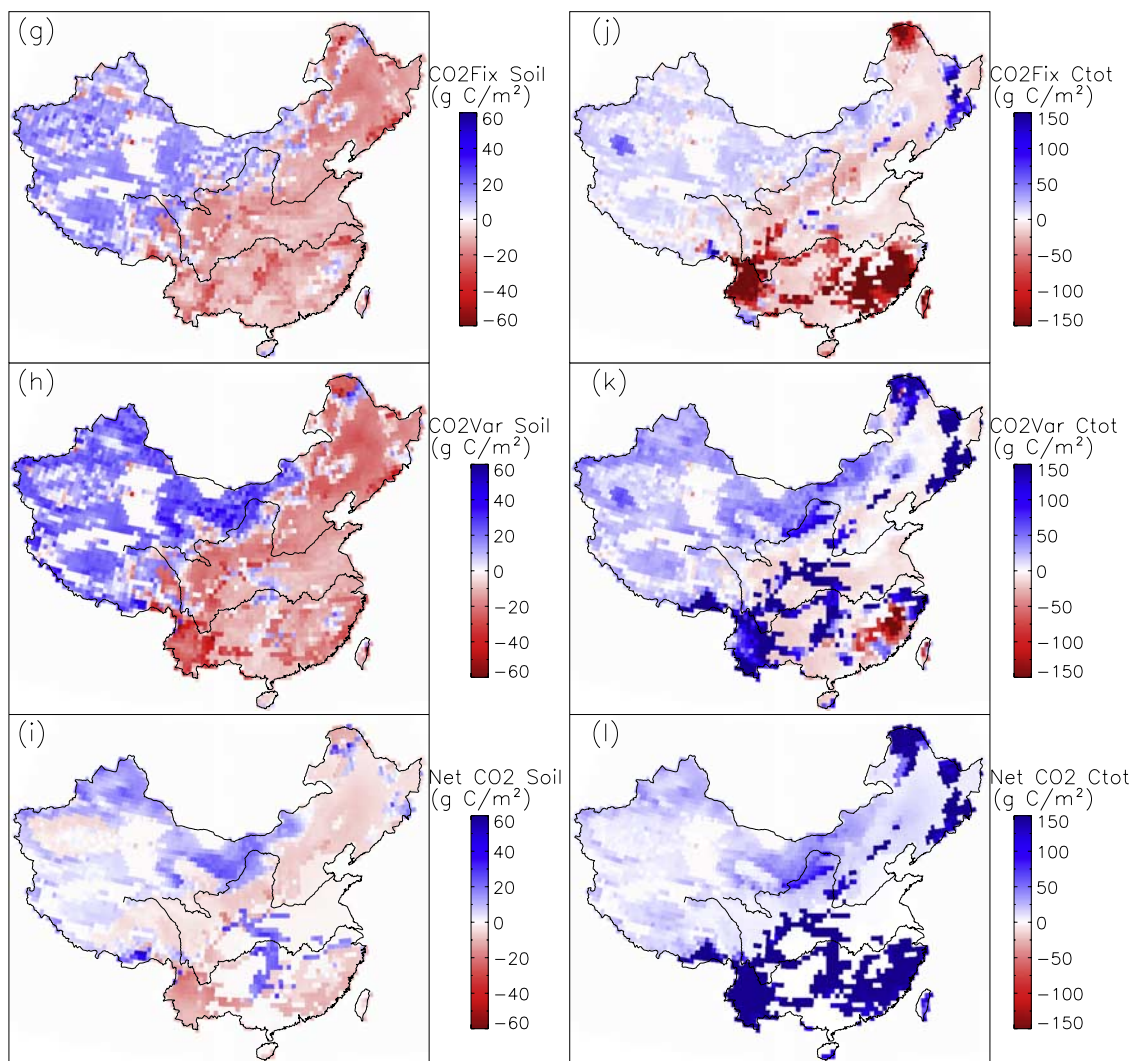
Figure 7. (continued)

NPP of 183.58 Tg C/a over results from climate alone, and increasing Ctot by 33.24 Pg C (Table 2). At the national scale, the effects of future doubled CO$_2$ combined with projected climate change will benefit vegetation growth, leading to higher rates of the carbon cycle (NPP: +238.46 Tg C/a, Rh: +218.13 Tg C/a, NEP: +21.33 Tg C/a) than at present (Table 2), which fixes more carbon to Cveg (+3.73 Pg C) and Csoil (+7.66 Pg C) but less Clitr (−1.76 Pg C less) in the future. The lower Clitr is caused by the higher litter decomposition rate, induced by the increasing temperature and precipitation (Figure 9). The Ctot will increase by 9.64 Pg C relative to the present (Figure 4 and Table 2).

3.2.2. Dynamic Spatial Changes in the Carbon Cycle

[38] In response to climate change and doubled CO$_2$, NPP will increase nearly all over China with the exception of southern China, where precipitation and temperature are high (Figure 10a). This may result from the assumptions that relative humidity (RH) is set to be as same as during the present. The increasing temperature increases saturated vapor pressure and hence increases VPD, which reduces stomatal conductance [*Sandford and Jarvis*, 1986; *Schulze*
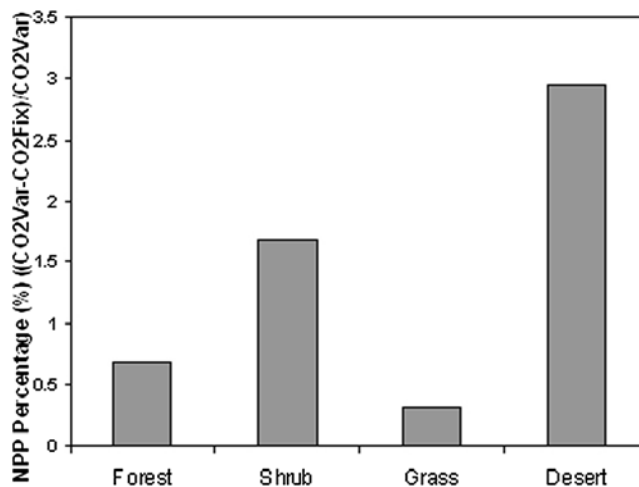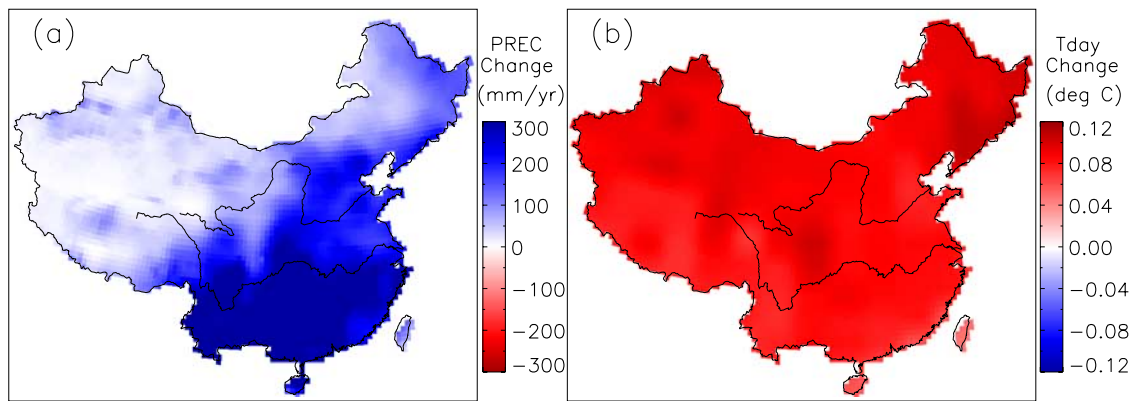

Figure 8. Percentage of net CO$_2$ fertilization effects on NPP (CO2Var − CO2Fix) as compared to the NPP average from CO2Var.

Figure 9. Projected future spatial changes with projected climate change under doubled CO_2 (2071–2110) in (a) precipitation (PREC) and (b) daytime temperature (Tday) under doubled CO_2 generated by Hadley Centre HadCM3 for the IPCC Fourth Assessment relative to the 1961–2000 observations.

et al., 1994; *Leuning*, 1995; *Oren et al.*, 1999; *Xu and Baldocchi*, 2002; *Mu et al.*, 2007]. This will offset the beneficial effects of increasing precipitation (Figure 9a) and radiation on NPP. Western China, the driest region in China, where xeric biomes dominate, has very low precipitation and high daytime temperature during the growing season. Increasing precipitation will decrease water stress significantly, leading to longer growing seasons, favoring terrestrial production, and increasing NPP. The average NPP there at the present is less than 100 g $C/m^2/a$, and the future NPP will increase with a similar magnitude to that of east China (Figures 2c and 10a), which indicates more significant stimulated vegetation growth in western China than in east China.

[39] The change in Cveg is positively related to changes in accumulated NPP each year, and the spatial pattern is similar to that of NPP (Figures 10a and 10c). Increasing air temperature and precipitation will increase soil temperature and soil moisture, respectively, which in turn enhance the litter decomposition to soils and Rh. NEP will increase in western China and decrease in east China (Figure 10b) averaged over the two time periods. Although coarse wood debris and the carbon transferred from vegetation to litter will increase in many parts of China, Clitr will be reduced over most of southeastern China (Figure 10d) in the future because of higher rates of litter decomposition to soils induced by warmer and wetter soils. A similar explanation can be applied to the change in Csoil over large areas of Central and east China, where Csoil will decrease (Figure 10e) as a result of higher soil respiration rates. As a combined result of changes in Cveg, Clitr and Csoil, Ctot will decrease in most parts of eastern China (Figure 10f). Despite the reduced Ctot in eastern China, at the national level, the future Ctot will be higher than the present (Figure 4 and Table 2), because it will increase by about 5 Kg C/m^2 in most parts of western China (Figure 10f), where the average Ctot is less than 12 Kg C/m^2 at the present.

4. Discussion

[40] This study uses a process-based ecosystem model, Biome-BGC and daily meteorological data, to examine the different roles of CO_2 fertilization effects and climate change in regulating dynamics of carbon fluxes and storages of China's ecosystems for the present (1961–2000) and a projected future climate scenario under doubled CO_2. However, there are three uncertainties in our study.

[41] First, our study concentrated on how atmospheric CO_2 and climate affect the carbon cycle for terrestrial China. As mentioned before, we didn't consider land use change resulted from human activities [*Tian et al.*, 2008], disturbances such as fires [*Lü et al.*, 2006; *Running*, 2006], and environmental pollution as aerosols [*Bergin et al.*, 2001], nitrogen deposition [*Sala et al.*, 2000] and O_3 [*Karnosky et al.*, 1999, 2002], which are important factors affecting ecosystem dynamics, and associated carbon budget in China, particularly in populated eastern China [*Tian et al.*, 2008; *Liu et al.*, 2005].

[42] Secondly, although our results agree with many other studies tested in large stature forests at realistic spatial and temporal scales using FACE technology [*Strain and Bazzaz*, 1983; *Hendrey and Kimball*, 1994; *Hendrey et al.*, 1999; *Moore et al.*, 2006], researchers still have limited knowledge of the responses of ecosystems to elevated CO_2 [*Luo et al.*, 1999; *Nowak et al.*, 2004; *Ainsworth and Long*, 2005; *Asshoff et al.*, 2006]. Some studies suggested that nitrogen availability may limit the CO_2 fertilization under

Table 2. Changes in Average Carbon Storages and Fluxes in the Future (2071–2110) Relative to the Average Over 1961–2000 at the National Scale From Two Sets of Biome-BGC Experiments[a]

Variables	Experiments		Net CO₂ Effects
	CO21X	CO22X	
Cveg change, Pg C/a	−5.57	3.73	9.31
Clitr change, Pg C/a	−5.04	−1.76	3.28
Csoil change, Pg C/a	−12.99	7.66	20.65
Ctot change, Pg C/a	−23.60	9.64	33.24
NPP change, Tg C/a	54.88	238.46	183.58
Rh change, Tg C/a	67.54	218.14	150.59
NEP change, Tg C/a	−11.66	21.33	32.99

[a]Variables are as in Table 1. Biome-BGC simulations are CO21X (fixed CO_2 as the average over 1961–2000 and future projected climate change) and CO22X (doubled CO_2 and future projected climate change).
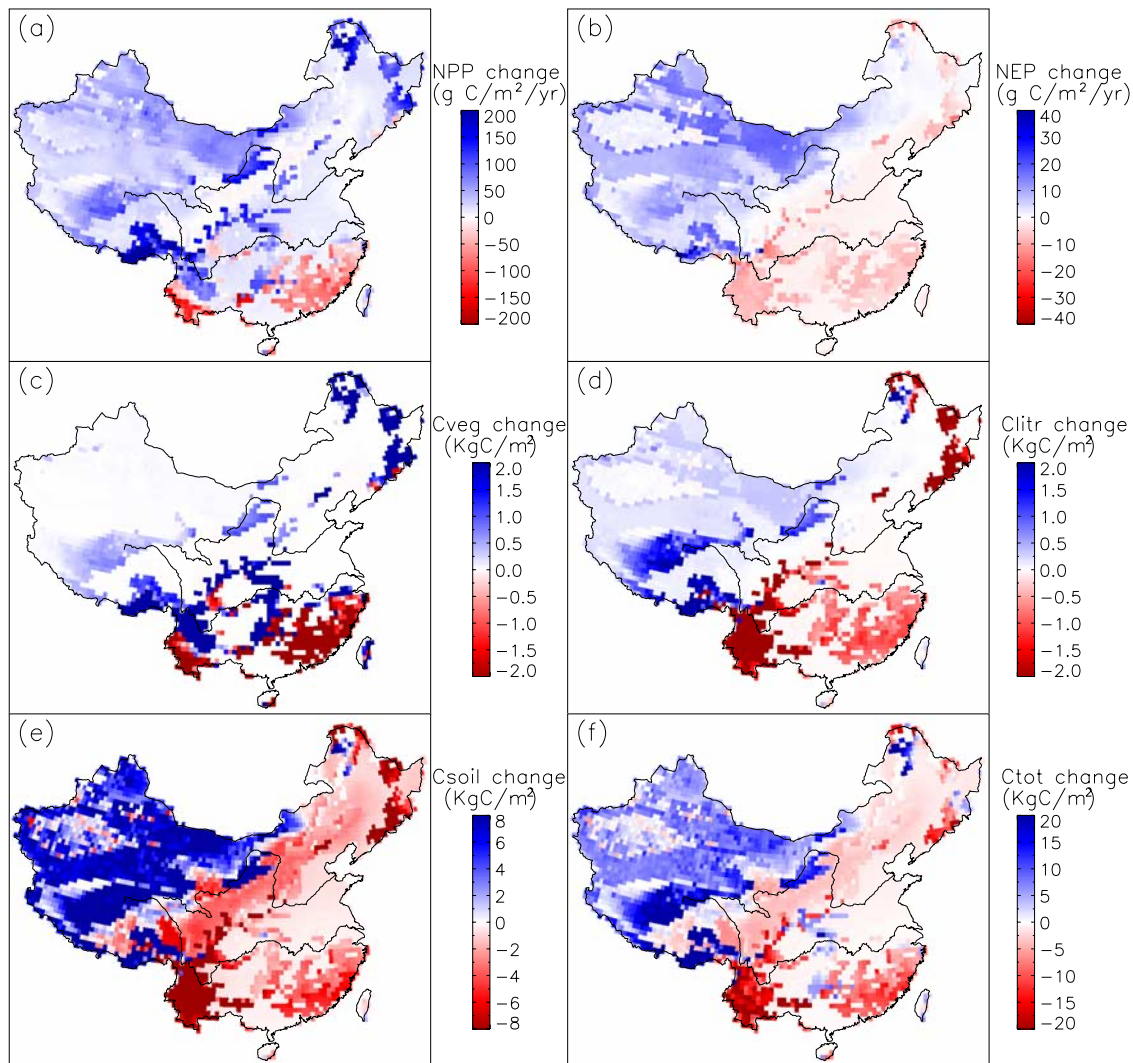
Figure 10. Future spatial changes with projected climate change under doubled CO_2 (2071–2110) in (a) NPP, (b) NEP, (c) vegetation carbon (Cveg), (d) litter carbon (Clitr), (e) soil carbon (Csoil), and (f) total carbon (Ctot) simulated by CO22X (doubled CO_2 and projected future climate under doubled CO_2 by Hadley Centre HadCM3 for the IPCC Fourth Assessment) relative to the present (CO2Var, driven by variable CO_2 concentration and observed meteorology, 1961–2000) for terrestrial China.

elevated CO_2 concentration [*Curtis et al.*, 2000; *Poorter and Pérez-Soba*, 2001; *Nowak et al.*, 2004; *Ainsworth and Long*, 2005]. Among 11 FACE sites, NPP was increased, while decreased NPP under elevated CO_2 only occurred with three different experiments in grasslands, which appeared to be statistical outliers [*Nowak et al.*, 2004]. *Ainsworth and Long* [2005] reviewed different FACE and chamber experiments. The decrease in nitrogen, often assumed to lead to an expected diminution of the response of vegetation to elevated CO_2 in the long term, is only marginal in FACE. *Oren et al.* [2001] reported that fertility, in particular nitrogen, could restrain the response of wood carbon sequestration to increased atmospheric CO_2 from a FACE experiment. However, *Moore et al.* [2006] analyzed the longer data record of the FACE experiment at the same site, concluding that there was no evidence of a systematic reduction in the

stimulation of growth during the first 8 years of this experiment, suggesting that the hypothesized limitation of the CO_2 response caused by nitrogen availability has yet to occur. Other studies reveal that elevated CO_2 causes net nitrogen accumulation in plant and soil pools, which may prevent complete down regulation of long-term CO_2 stimulation of carbon sequestration [*Luo et al.*, 2006a, 2006b]. The many large differences between the findings within FACE and prior chamber experiments clearly show the need for a wider use of FACE, and most importantly side-by-side experiments to separate technique from site difference. Therefore we still have not fully understood the role of nitrogen supply in CO_2 fertilization effects. For the current version of Biome-BGC, there is no nitrogen constraint for stimulated photosynthesis by CO_2 fertilization effects [*Thornton*, 1998], which might introduce some bias.

[43] Thirdly, water availability also has impacts on the response of ecosystems to elevated CO_2. The early conceptual model of *Strain and Bazzaz* [1983] suggested that CO_2 fertilization be greater for xeric ecosystems or in dry years within an ecosystem. However, FACE experiments do not fully support this prediction [*Nowak et al.*, 2004]. Generally, most FACE experiments show that CO_2 fertilization effects increase with increasing precipitation for both forests and grasslands, and are greater for forests than grasslands [*Nowak et al.*, 2004]. More research is needed to solve this discrepancy.

[44] Finally, we used one model to estimate the effects of CO_2 fertilization and climate change, while the descriptions of photosynthesis processes in other ecosystem models are different [*Pan et al.*, 1998]. Therefore, for a given region, different models may generate different results. For example, *Schimel et al.* [2000] found that within the conterminous USA, for some regions, differences in net carbon storage estimated by three biogeochemical models could reach a factor of three. In addition, different GCMs may have different projected climate changes under doubled CO_2, which may pose limitations on our conclusions for the future estimates. We used the projected climate change by only one GCM (HadCM3) because HadCM2 has the best performance for China among several GCMs [*Zhao et al.*, 2002]. There are also large uncertainties in the projected climate change, which is beyond the scope of our study. Because the climate data are the same for the different two simulations both at present and in the future, respectively, the uncertainties in the projected future climate change should not significantly change the effects of CO_2 fertilization simulated by Biome-BGC.

5. Conclusions

[45] This study examines the different roles of CO_2 fertilization effects and climate change in regulating the dynamics of carbon fluxes and storages of China's ecosystems for the present (1961–2000) and projected future climate scenarios under doubled CO_2. The CO_2 fertilization effects enhanced NPP for nearly all of China during 1961–2000. On average, the NPP enhancement by the CO_2 fertilization effects was greatest in deserts, lowest in grasslands with shrub and forest intermediate, which generally agrees with the FACE results [*Nowak et al.*, 2004]. Though the accuracy of the absolute values of our estimated carbon fluxes and storages is a separate issue because of the uncertainties mentioned above, the relative values reveal that at the national scale, total carbon storage in China's ecosystems will decrease (increase) without (with) incorporating elevated CO_2 fertilization effects for both the present and the future with projected climate change. The CO_2 fertilization effects caused by elevated CO_2 may compensate for the adverse effects of climate change which is largely induced by increasing atmospheric greenhouse gases, especially CO_2, on some ecosystems, like on China's ecosystems.

References

Ainsworth, E. A., and S. P. Long (2005), What have we learned from 15 years of free-air CO_2 enrichment (FACE)? A meta-analytic review of the responses of photosynthesis, canopy properties and plant production to rising CO_2, *New Phytol.*, *165*, 351–372.

Allan, R. P., M. A. Ringer, and A. Slingo (2003), Evaluation of moisture in the Hadley Centre climate model using simulations of HIRS water-vapour channel radiances, *Q. J. R. Meteorol. Soc.*, *129*, 3371–3389.

Amthor, J. S. (2000), The McCree–de Wit–Penning de Vries–Thornley respiration paradigms: 30 years later, *Ann. Bot.*, *86*, 1–20.

Asshoff, R., G. Zotz, and C. Körner (2006), Growth and phenology of mature temperate forest trees in elevated CO_2, *Global Change Biol.*, *12*, 848–861.

Bergin, M. H., R. Greenwald, J. Xu, Y. Berta, and W. L. Chameides (2001), Influence of aerosol dry deposition on photosynthetically active radiation available to plants: A case study in the Yangtze delta region of China, *Geophys. Res. Lett.*, *28*, 3605–3608.

Black, T. A., W. J. Chen, A. G. Barr, M. A. Arain, Z. Chen, Z. Nesic, E. H. Hogg, H. H. Neumann, and P. C. Yang (2000), Increased carbon sequestration by a boreal deciduous forest in years with a warm spring, *Geophys. Res. Lett.*, *27*, 1271–1274.

Cao, M. K., S. D. Prince, K. Li, B. Tao, J. Small, and X. Shao (2003), Response of terrestrial carbon uptake to climate interannual variability in China, *Global Change Biol.*, *9*, 536–546.

Chen, J. M., B. Chen, K. Higuchi, J. Liu, D. Chan, D. Worthy, P. Tans, and A. Black (2006), Boreal ecosystems sequestered more carbon in warmer years, *Geophys. Res. Lett.*, *33*, L10803, doi:10.1029/2006GL025919.

Churkina, G., and S. W. Running (1998), Contrasting climatic controls on the estimated productivity of different biomes, *Ecosystems*, *1*, 206–215.

Curtis, P. S., and X. Wang (1998), A meta-analysis of elevated CO_2 effects on woody plant mass, form, and physiology, *Oecologia*, *113*, 299–313.

Curtis, P. S., C. S. Vogel, X. Wang, K. S. Pregitzer, D. R. Zak, J. Lussenhop, M. Kubiske, and J. A. Teeri (2000), Gas exchange, leaf nitrogen, and growth efficiency of *Populus tremuloides* in a CO_2-enriched atmosphere, *Ecol. Appl.*, *10*, 3–17.

DeLucia, E. H., D. J. Moore, and R. J. Norby (2005), Contrasting responses of forest ecosystems to rising atmospheric CO_2: Implications for the global C cycle, *Global Biogeochem. Cycles*, *19*, GB3006, doi:10.1029/2004GB002346.

De Pury, D. G. G., and G. D. Farquhar (1997), Simple scaling of photosynthesis from leaves to canopies without the errors of big-leaf models, *Plant Cell Environ.*, *20*, 537–557.

Fang, J., S. Piao, C. B. Field, Y. Pan, Q. Guo, L. Zhou, C. Peng, and S. Tao (2003), Increasing net primary production in China from 1982 to 1999, *Frontiers Ecol. Environ.*, *1*(6), 293–297.

Fang, J. Y., A. P. Chen, C. H. Peng, S. Q. Zhao, and L. Ci (2001), Changes in forest biomass carbon storage in China between 1949 and 1998, *Science*, *292*, 2320–2322.

Farquhar, G. D., S. von Caemmerer, and J. A. Berry (1980), A biochemical model of photosynthetic CO_2 assimilation in leaves of C3 species, *Planta*, *149*, 78–90.

Farquhar, G. D., S. von Caemmerer, and J. A. Berry (2001), Models of photosynthesis, *Plant Physiol*, *125*, 42–45.

Friedl, M. A., et al. (2002), Global land cover mapping from MODIS: Algorithms and early results, *Remote Sens. Environ.*, *83*, 287–302.

Friedlingstein, P., I. Fung, E. Holland, J. John, G. Brasseur, D. Erickson, and D. Schimel (1995), On the contribution of CO_2 fertilization to the missing biospheric sink, *Global Biogeochem. Cycles*, *9*, 541–556.

Gifford, R. M. (1994), The global carbon cycle: A viewpoint on the missing sink, *Aust. J. Plant Physiol.*, *21*, 1–15.

Graaff, M.-A., K.-J. Groenigen, J. Six, B. Hungate, and C. Kessel (2006), Interactions between plant growth and soil nutrient cycling under elevated CO_2: A meta-analysis, *Global Change Biol.*, *12*, 2077–2091.

Hendrey, G. R., and B. A. Kimball (1994), The FACE program, *Agric. For. Meteorol.*, *70*, 3–14.

Hendrey, G. R., D. S. Ellsworth, K. F. Lewin, and J. Nagy (1999), A free-air enrichment system for exposing tall forest vegetation to elevated atmospheric CO_2, *Global Change Biol.*, *5*, 293–309.

Ingram, W. J. (2002), On the robustness of the water vapor feedback: GCM vertical resolution and formulation, *J. Clim.*, *15*, 917–921.

Intergovernmental Panel on Climate Change (IPCC) (2001), The science of climate change, in *Climate Change 2001: The Scientific Basis, Contribution of Working Group I to the Third Assessment Report of the Intergovernmental Panel on Climate Change*, edited by J. T. Houghton, et al., pp. 156–159, Cambridge Univ. Press, New York.

Intergovernmental Panel on Climate Change (IPCC) (2007), *Climate Change 2007: The Scientific Basis: Contribution of Working Group I to the Fourth Assessment Report of the Intergovernmental Panel on Climate Change*, edited by S. Solomon, et al., Cambridge Univ., Press, New York.

Kaiser, D. P., and Y. Qian (2002), Decreasing trends in sunshine duration over China for 1954–1998: Indication of increased haze pollution?, *Geophys. Res. Lett.*, *29*(21), 2042, doi:10.1029/2002GL016057.

Karl, T. R., G. Kukla, V. N. Razuvayev, M. J. Changery, R. G. Quayle, R. R. Heim Jr., D. R. Easterling, and C. B. Fu (1991), Global warming: Evidence for asymmetric diurnal temperature change, *Geophys. Res. Lett.*, *18*, 2253–2256.

Karl, T. R., P. D. Jones, R. W. Wright, G. Kukla, N. Plummer, V. Razuvayev, K. P. Gallo, J. Lindseay, R. J. Charlson, and T. C. Peterson (1993), A new perspective on recent global warming: Asymmetric trends of daily maximum and minimum temperature, *Bull. Am. Meteorol. Soc.*, *74*(6), 1007–1023.

Karnosky, D. F., et al. (1999), Effects of tropospheric O₃ on trembling aspen and interaction with CO₂: Results from an O₃-gradient and a FACE experiment, *Water Air Soil Pollut.*, *116*, 311–322.

Karnosky, D. F., et al. (2002), Tropospheric O₃ moderate responses of temperate hardwood forests to elevated CO₂: A synthesis of molecular to ecosystem results from the Aspen FACE project, *Funct. Ecol.*, *17*, 289–304.

Keeling, C. D., T. P. Whorf, M. Wahlen, and J. van der Plicht (1995), Interannual extremes in the rate of rise of atmospheric carbon dioxide since 1980, *Nature*, *375*, 660–670.

Kimball, J., S. W. Running, and R. Nemani (1997), An improved method for estimating surface humidity from daily minimum temperature, *Agric. For. Meteorol.*, *85*, 87–98.

Leuning, R. (1995), A critical appraisal of a combined stomatal-photosynthesis model for C3 plants, *Plant Cell Environ.*, *18*, 55–339.

Lewis, J. D., X. Z. Wang, K. L. Griffin, and D. T. Tissue (2002), Effects of age and ontogeny on photosynthetic responses of a determinate annual plant to elevated CO₂ concentrations, *Plant Cell Environ.*, *25*, 359–368, doi:10.1046/j.0016-8025.2001.00815.x.

Liu, J., H. Tian, M. Liu, D. Zhuang, J. M. Melillo, and Z. Zhang (2005), China's changing landscape during the 1990s: Large-scale land transformation estimated with satellite data, *Geophys. Res. Lett.*, *32*, L02405, doi:10.1029/2004GL021649.

Lloyd, J., and J. A. Taylor (1994), On the temperature dependence of soil respiration, *Funct. Ecol.*, *8*, 315–323.

Lü, A., H. Tian, M. Liu, J. Liu, and J. M. Melillo (2006), Spatial and temporal patterns of carbon emissions from forest fires in China from 1950 to 2000, *J. Geophys. Res.*, *111*, D05313, doi:10.1029/2005JD006198.

Luo, Y., J. Reynolds, Y. Wang, and D. Wolfe (1999), A search for predictive understanding of plant responses to elevated [CO₂], *Global Change Biol.*, *5*, 143–156.

Luo, Y., C. B. Field, and R. B. Jackson (2006a), Does nitrogen constrain carbon cycling, or does carbon input stimulate nitrogen cycling?, *Ecology*, *87*, 3–4.

Luo, Y., D. Hui, and D. Zhang (2006b), Elevated CO₂ stimulates net accumulations of carbon and nitrogen in land ecosystems: A meta-analysis, *Ecology*, *87*, 53–63.

Ma, Z. G. (1999), The relationship between soil moisture and regional climate change in east China and an inverse model for the soil moisture, Ph.D. dissertation, Inst. of Atmos. Phys., Chin. Acad. of Sci., Beijing.

McGuire, A. D., et al. (2001), Carbon balance of the terrestrial biosphere in the twentieth century: Analyses of CO₂, climate and land use effects with four process-based ecosystem models, *Global Biogeochem. Cycles*, *15*, 183–206.

McNeill, J. R. (2000), *Something New Under the Sun: An Environmental History of the Twentieth-Century World*, 421 pp., W. W. Norton, New York.

Melillo, J. M., A. D. McGuire, D. W. Kicklighter, B. Moore, C. J. Vorosmarty, and A. L. Schloss (1993), Global climate change and terrestrial net primary production, *Nature*, *363*, 234–240.

Moore, D. J. P., S. Aref, R. M. Ho, J. S. Pippen, J. G. Hamilton, and E. H. De Lucia (2006), Annual basal area increment and growth duration of *Pinus taeda* in response to eight years of free-air carbon dioxide enrichment, *Global Change Biol.*, *12*, 1367–1377.

Mu, Q., M. Zhao, F. A. Heinsch, M. Liu, H. Tian, and S. W. Running (2007), Evaluating water stress controls on primary production in biogeochemical and remote sensing based models, *J. Geophys. Res.*, *112*, G01012, doi:10.1029/2006JG000179.

Nemani, R., C. D. Keeling, H. Hashimoto, W. M. Jolly, S. C. Piper, C. J. Tucker, R. B. Myneni, and S. W. Running (2003), Climate-driven increases in global terrestrial net primary production from 1982 to 1999, *Science*, *300*, 1560–1563.

Norby, R. J., et al. (2005), Forest response to elevated CO₂ is conserved across a broad range of productivity, *Proc. Natl. Acad. Sci. U. S. A.*, *102*(50), 18,052–18,056.

Nowak, R. S., D. S. Ellsworth, and S. D. Smith (2004), Functional responses of plants to elevated atmospheric CO₂—Do photosynthetic and productivity data from FACE experiments support early predictions?, *New Phytol.*, *162*, 253–280.

Oren, R., J. S. Sperry, G. G. Katul, D. E. Pataki, B. E. Ewers, N. Phillips, and K. V. R. Schäfer (1999), Survey and synthesis of intra- and interspecific variation in stomatal sensitivity to vapour pressure deficit, *Plant Cell Environ.*, *22*, 1515–1526.

Oren, R., et al. (2001), Soil fertility limits carbon sequestration by forest ecosystems in a CO₂-enriched atmosphere, *Nature*, *411*, 469–478.

Pan, Y., J. M. Melillo, A. D. McGuire, D. W. Kicklighter, L. Pitelka, and VEMAP members (1998), Modeled responses of terrestrial ecosystems to elevated atmospheric CO₂: A comparison of simulations by the biogeochemistry models of Vegetation/Ecosystem Model and Analysis Project (VEMAP), *Oecologia*, *114*, 389–402.

Poorter, H., and M. Pérez-Soba (2001), The growth response of plants to elevated CO₂ under non-optimal environmental conditions, *Oecologia*, *129*, 1–20.

Prentice, I. C., et al. (2001), The carbon cycle and atmospheric carbon dioxide, in *Climate Change 2001: The Scientific Basis: Contribution of Working Group I to the Third Assessment Report of the Intergovernmental Panel on Climate Change*, edited by J. T. Houghton et al., pp. 182–237, Cambridge Univ. Press, New York.

Raich, J. W., E. B. Rastetter, J. M. Mellilo, D. W. Kicklighter, P. A. Steudler, B. J. Peterson, A. L. Grace, B. Moore III, and C. J. Vorosmarty (1991), Potential net primary productivity in South America: Application of a global model, *Ecol. Appl.*, *1*, 399–429.

Roderick, M. L., and G. D. Farquhar (2002), The cause of decreased pan evaporation over the past 50 years, *Science*, *298*, 1410–1411.

Running, S. W. (2006), Is global warming causing more, larger wildfires?, *Science*, *313*, 927–928, doi:10.1126/science.1130370.

Running, S. W., and E. R. Hunt (1993), Generalization of a forest ecosystem process model for other biomes, Biome-BGC, and an application for global-scale models, in *Scaling Physiological Processes: Leaf to Globe*, edited by J. R. Ehleringer and C. B. Field, pp. 141–158, Academic, San Diego, Calif.

Running, S. W., and J. S. Kimball (2005), Satellite-based analysis of ecological controls for land-surface evaporation resistance, in *Encyclopedia of Hydrological Sciences*, vol. 3, edited by M. Anderson, chap. 104, pp. 1587–1600, John Wiley, Hoboken, N. J.

Ryan, M. G. (1991), The effects of climate change on plant respiration, *Ecol. Appl.*, *1*, 157–167.

Sabine, C. L., et al. (2004), Current status and past trends of the global carbon cycle, in *The Global Carbon Cycle: Integrating Humans, Climate, and the Natural World*, SCOPE, vol. 62, edited by C. B. Field and M. R. Raupach, pp. 17–44, Island, Washington, D. C.

Sala, O. E., et al. (2000), Global biodiversity scenarios for the year 2100, *Science*, *287*, 1770–1774.

Sandford, A. P., and P. G. Jarvis (1986), Stomatal responses to humidity in selected conifers, *Tree Physiol.*, *2*, 89–103.

Schimel, D., et al. (2000), Contribution of increasing CO₂ and climate to carbon storage by ecosystems in the United States, *Science*, *287*, 2004–2006.

Schulze, E. D., F. M. Kelliher, C. Körner, J. Lloyd, and R. Leuning (1994), Relationships among maximum stomatal conductance, ecosystem surface conductance, carbon assimilation rate, and plant nitrogen nutrition: A global ecology scaling exercise, *Annu. Rev. Ecol. Syst.*, *25*, 629–660.

Seneviratne, S. I., J. S. Pal, E. A. B. Eltahir, and C. Schar (2002), Summer dryness in a warmer climate: A process study with a regional climate model, *Clim. Dyn.*, *20*, 69–85.

Sims, P. L., and P. G. Risser (1999), Grasslands, in *North American Terrestrial Vegetation*, edited by M. G. Barbour and W. D. Billings, pp. 323–356, Cambridge Univ. Press, New York.

State Statistical Bureau (2003), *Statistical Yearbook of China*, China Stat. Publ. House, Beijing.

Strain, B. R., and F. A. Bazzaz (1983), Terrestrial plant communities, in *CO₂ and Plants: The Response of Plants to Rising Levels of Atmospheric Carbon Dioxide*, edited by E. R. Lemon, pp. 177–222, Westview, Boulder, Colo.

Thornton, P. E. (1998), Regional ecosystem simulation: Combining surface- and satellite-based observations to study linkages between terrestrial energy and mass budgets, Ph.D. dissertation, 280 pp., Sch. of For., Univ. of Mont., Missoula.

Thornton, P. E., and S. W. Running (1999), An improved algorithm for estimating incident daily solar radiation from measurements of temperature, humidity, and precipitation, *Agric. For. Meteorol.*, *93*, 211–228.

Thornton, P. E., S. W. Running, and M. A. White (1997), Generating surfaces of daily meteorology variables over large regions of complex terrain, *J. Hydrol.*, *190*, 214–251.

Thornton, P. E., et al. (2002), Modeling and measuring the effects of disturbance history and climate on carbon and water budgets in evergreen needleleaf forests, *Agric. For. Meteorol.*, *113*, 185–222.

Tian, H., J. M. Melillo, D. W. Kicklighter, A. D. McGuire, J. Helfrich, B. Moore III, and C. J. Vörösmarty (1998), Effect of interannual climate variability on carbon storage in Amazonian ecosystems, *Nature*, *396*, 664–667.

Tian, H., et al. (1999), The sensitivity of terrestrial carbon storage to historical atmospheric CO_2 and climate variability in the United States, *Tellus, Ser. B*, *51*, 414–452.

Tian, H., et al. (2003), Regional carbon dynamics in monsoon Asia and its implications for the global carbon cycle, *Global Planet. Change*, *37*, 201–217.

Tian, H., et al. (2008), The terrestrial carbon budget in east Asia: Human and natural impacts, in *Changes in the Human-Monsoon System of East Asia in the Context of Global Change*, *SCOPE*, edited by C. Fu, J. Freney, and J. Steward, Island, Washington, D.C., in press.

Wang, Q., M. Watanabe, and Z. Ouyang (2005), Simulation of water and carbon fluxes using Biome-BGC model over crops in China, *Agric. For. Meteorol.*, *131*, 209–224.

Wang, S., et al. (2003), Pattern and change in soil organic carbon storage in China: 1960s–1980s, *Tellus, Ser. B*, *55*, 416–427.

White, M. A., P. E. Thornton, and S. W. Running (1997), A continental phenology model for monitoring vegetation responses to interannual climatic variability, *Global Biogeochem. Cycles*, *11*, 217–234.

White, M. A., et al. (2000), Parameterization and sensitivity analysis of the BIOME_BGC terrestrial ecosystem model: Net primary production controls, *Earth Interact.*, *4*(3), 1–84.

Wittig, V. E., C. J. Bernacchi, X. G. Zhu, C. Calfapietra, R. Ceulemans, P. Deangelis, B. Gielen, F. Miglietta, P. B. Morgan, and S. P. Long (2005), Gross primary production is stimulated for three *Populus* species grown under free-air CO_2 enrichment from planting through canopy closure, *Global Change Biol.*, *11*, 644–656.

Woodrow, I. E., and J. A. Berry (1988), Enzymatic regulation of photosynthetic CO_2 fixation in C3 plants, *Annu. Rev. Plant Physiol. Plant Mol. Biol.*, *39*, 533–594.

Wullschleger, S. D. (1993), Biochemical limitations to carbon assimilation in C3 plants—A retrospective analysis of the A/Ci curves from 109 species, *J. Exp. Bot.*, *44*, 907–920, doi:10.1093/jxb/44.5.907.

Xu, L., and D. D. Baldocchi (2002), Seasonal trend of photosynthetic parameters and stomatal conductance of blue oak (*Quercus douglasii*) under prolonged summer drought and high temperature, *Tree Physiol.*, *23*, 865–877.

Ye, B., A. D. Del Genio, and K. K. W. Lo (1998), CAPE variations in the current climate and in a climate change, *J. Clim.*, *11*, 1997–2015.

Zhai, P. M., and X. Pan (2003), Trends in temperature extremes during 1951–1999 in China, *Geophys. Res. Lett.*, *30*(17), 1913, doi:10.1029/2003GL018004.

Zhai, P. M., F. M. Ren, and Q. Zhang (1999), Detection of trends in China's precipitation extremes, *Acta Meteorol. Sin.*, *57*, 208–216.

Zhang, C., H. Q. Tian, J. Liu, S. Wang, M. Liu, S. Pan, and X. Shi (2005), Pools and distributions of soil phosphorus in China, *Global Biogeochem. Cycles*, *19*, GB1020, doi:10.1029/2004GB002296.

Zhao, M., R. Neilson, X. Yan, and W. Dong (2002), Modelling the vegetation of China under changing climate, *Acta Geogr. Sin.*, *57*(1), 28–38.

─────────────────

M. Liu and H. Tian, School of Forestry and Wildlife Sciences, Auburn University, Auburn, AL 36849, USA.

Q. Mu, S. W. Running, and M. Zhao, Numerical Terradynamic Simulation Group, College of Forestry and Conservation Sciences, University of Montana, Missoula, MT 59812, USA (qiaozhen@ntsg.umt.edu; zhao@ntsg.umt.edu)